Ammonia Adsorption on Keggin-Type Heteropolyacid Catalysts Explored by Density Functional Quantum Chemistry Calculations

Billy B. Bardin, Robert J. Davis, and Matthew Neurock*

Department of Chemical Engineering, University of Virginia, Charlottesville, Virginia 22903-2442

Received: September 13, 1999; In Final Form: January 26, 2000

Density functional quantum chemical calculations have been used to compare the acid strengths of phosphotungstic and phosphomolybdic acids by computing the adsorption energy of ammonia on model clusters of each heteropolyacid. The adsorption of ammonia on a phosphotungstic acid cluster was stronger than the adsorption on a phosphomolybdic acid cluster. The predicted adsorption energies were near −150 and −106 kJ mol^{-1} for phosphotungstic and phosphomolybdic acid, respectively. This compares well with the experimental heats of ammonia sorption determined from microcalorimetry. An analysis of different adsorption modes of ammonia on phosphotungstic acid showed that bidentate adsorption of ammonia on the heteropolyacid clusters aided in proton transfer and yielded stronger adsorption energies than did a monodentate adsorption mode. In addition, we report the computed adsorption energies of pyridine on a heteropolyacid cluster.

Introduction

The drive to develop environmentally friendly chemical processes has motivated a significant increase in research activities that encompass understanding and designing solid acid catalysts. These materials offer the unique opportunity to replace the corrosive liquid acids currently used in many chemical conversion steps to provide "greener" processes. The replacement of liquid acids with solid acid catalysts also simplifies downstream processing because no separation is needed to recover the acid catalyst. Many materials have been used as solid acid catalysts including clays, zeolites, sulfated and tungstated zirconia, and heteropolyacids.[1] Each of these materials offers unique structural and chemical differences that can markedly influence the acid chemistry. Zeolites, for example, are excellent candidates for shape-selective chemistry because of their well-defined pore structure.

Understanding the interaction of molecules with the acid sites in these solid acid materials provides insight into the fundamental chemistry. Discovering which technique provides the best measure of solid acid strength has been a matter of dispute for many years. As discussed in a recent paper,[2] techniques such as temperature-programmed desorption, ^{1}H NMR, microcalorimetry, and catalytic probe reactions have all been used as alternatives to the controversial Hammett indicators to measure solid acidity. Quantum chemical methods have also been used to model solid acidity. Two specific methods exist for modeling acid strength. The first method involves calculating the proton affinity of the catalyst model as a theoretical measure of site strength.[3−5] However, there is no easy method to experimentally determine solid acid proton affinity and, thus, no way to compare computed values to experimental results. The second method that exists to probe acid site strength involves the calculation of adsorption energies of basic molecules such as ammonia and pyridine on a catalyst model.[6−11] These computed adsorption energies can be compared to the values determined from microcalorimetry.[12] Both approaches have been used effectively to help characterize acidity in zeolites. Many small-model clusters have been used to simulate the zeolite acid site, and in recent literature, embedded cluster models have been used to introduce the long-range effect of the zeolite cage on simulations of acid chemistry.[13,14] During these studies, various molecules have been used to computationally explore the acid chemistry of zeolites. Most common among these molecules are water, ammonia, and methanol.[15]

Herein, we have modeled the class of materials known as heteropolyacids (HPAs) using density functional theory (DFT) quantum chemical calculations. Heteropolyacids prove to be ideal from the computational standpoint because they have well-defined local structures.[16] In fact, the Keggin-type heteropolyacids have been examined using the extended Hückel theory.[17,18] Heteropolyacids are well-known strong acid catalysts, in both solution and solid forms,[19] and catalyze paraffin skeletal isomerization at low temperature.[20−22] The most common HPA is the Keggin-type, but many other structures are also known. These other structures, however, are thermally less stable and therefore not as useful for acid catalysis.[23] A schematic of the primary structure of the Keggin-type HPA is shown in Figure 1. The Keggin unit has the general formula $QM_{12}O_{40}^{x-}$, where Q is the central atom (usually phosphorus or silicon), M is a transition-metal atom (usually tungsten or molybdenum), and x is the charge on the primary structure. The Keggin unit is composed of a central tetrahedron surrounded by 12 transition-metal−oxygen octahedra. The central tetrahedron is formed from four oxygen atoms bonded to a central atom. Each transition-metal atom is bonded to six oxygen atoms to form the 12 octahedra on the outer-edge of the Keggin unit. Four types of oxygen atoms are found in the Keggin structure. These are the central oxygens, terminal oxygens, and two types of bridging oxygens. Central oxygen atoms bridge the central atom with the transition-metal atoms. The terminal oxygens form a double bond to a single transition-metal atom, whereas the bridging oxygen atoms form single bonds to two different transition-metal atoms.[16]

The acidity of heteropolyacids is Brønsted in nature. Keggin units with a phosphorus as the central atom and a tungsten or molybdenum as the transition metal atom will have a charge of −3. To balance the negative charge on the Keggin structure, protons or cations are needed.[23] The overall composition is then $H_3PM_{12}O_{40}$, where M = Mo or W. Heteropolyacids have not only a primary structure but also a secondary structure. The

* To whom correspondence should be addressed.

10.1021/jp993227t CCC: $19.00
Published on Web 03/21/2000

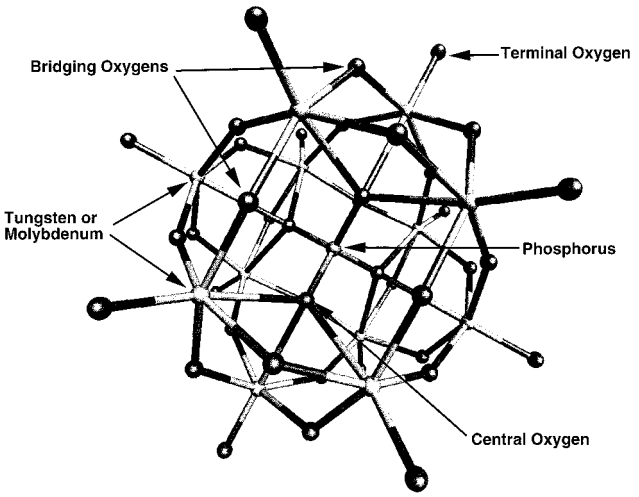

Figure 1. The Keggin unit contains a central atom (phosphorus), addenda atoms (tungsten or molybdenum), and three types of oxygen atoms (bridging, terminal, and central).

secondary structure is determined by the number of waters of hydration found in the solid.[19] Hydrogen bonds in a hydrated sample help to maintain the secondary structure. In the hydrous form, the protons are speculated to sit in the center of the secondary cavity between the water molecules, thus forming an $H_5O_2^+$ species.[24] In an anhydrous system, however, the position of the proton is not as well-known. Lee et al. concluded from infrared spectroscopy that protons were most likely located on bridging oxygens,[25] but others have suggested that the proton resides between two adjacent Keggin units hydrogen bonded to terminal oxygens.[26] In an earlier paper, we reported that the most energetically favorable position for the proton in an isolated, anhydrous heteropolyacid was the bridging oxygen, as determined from calculated proton affinities.[2]

In this paper, we have used density functional quantum chemical calculations to model the interactions of ammonia with an anhydrous Keggin unit. The results obtained from the DFT calculations are compared to previously reported experimental heats of ammonia sorption obtained from microcalorimetry.[2] We explicitly explore several possible adsorption configurations for ammonia on the Keggin structure to help establish the most favorable adsorption sites.

Computational Methods

Gradient corrected density functional quantum chemical calculations were performed to determine the adsorption energies of ammonia on the various clusters that represent the Keggin unit. The use of DFT methods to examine well-defined catalysts has increased dramatically in the past few years. Density functional methods offer levels of accuracy that compare with that of ab initio MP2 methods but at a significantly lower computational cost. Bond energies are typically determined to within about 20 kJ mol^{-1} and bond lengths to approximately 0.05 Å for well-defined organometallic systems.[27,28] The adsorption energies are defined as the difference in energy of the ammonia/HPA cluster minus the energy of the separate ammonia and cluster fragments as shown in eq 1.

$$\Delta E_{ads}^{NH_3} = E_{NH_3/cluster} - E_{NH_3} - E_{cluster} \qquad (1)$$

The calculations for all clusters examined in this work were computed using the Amsterdam density functional (ADF)[29−31] code on an IBM SP2 and a Silicon Graphics Origin 200. All of the calculations were performed in a manner whereby the entire structure including the cluster and the adsorbate were allowed to fully optimize to determine their corresponding energetics. The electronic structure for each cluster was determined by iterating on the density to solve the series of single-electron Kohn−Sham equations, thus providing a self-consistent solution. Analytical derivatives of the energy were computed at each SCF cycle and used to establish the relative changes in the nuclear coordinates for subsequent geometry optimization steps. All of the calculations were performed using the Vosko−Wilk−Nusair (VWN) exchange-correlation potential[32] with Becke[33,34] and Perdew[35] nonlocal gradient corrections for the correlation and exchange energies, respectively. The gradient corrections were included in each iteration of the self-consistent field cycle. The density and energy of each SCF cycle were converged to within 1×10^{-3} and 1×10^{-5} au, respectively. The geometries were optimized to within 1×10^{-3} au. Triple-ζ basis sets were employed for all atoms. The core electrons, up to and including the 4p, 5p, 2p, and 1s shells, were frozen for molybdenum, tungsten, phosphorus, and oxygen atoms, respectively. Scalar relativistic corrections were explicitly included via the frozen core potentials. Relativistic corrections, along with geometry optimizations, were required for reliable predictions of structure and energetics.

The clusters used in this paper were originally developed to aid in the calculation of the proton affinity of the Keggin-type heteropolyacids.[2] They are labeled as monomer, dimer, trimer, tetramer, and Keggin unit, for which the value in the name corresponds to the number of metal atoms found in the cluster. For example, the monomer has one tungsten or molybdenum atom, whereas the dimer has two metal atoms. The clusters are small parts of the Keggin unit. The missing bonds at the edge of the cluster have been terminated with hydrogen atoms to maintain neutrality. The Keggin unit is not a cluster, but instead, is the entire primary structure of the heteropolyacid. The clusters and structures were all fully optimized before ammonia was brought near to the surface. In this paper, we have only considered the interaction of ammonia with one of the three protons located on the Keggin unit. We expect that the protons will be will dispersed on the Keggin unit and, thus, will have little interaction with ammonia adsorbed on another acidic proton. However, there may be some changes in the partial charges on the Keggin unit that may need to be considered. Little change in surface structure was observed when ammonia was adsorbed on the structure. One advantage of modeling the Keggin-type heteropolyacid is the closed local structure. Unlike zeolites, which have long-range structures that must be considered in the computation, the Keggin unit encompasses the entire local structure. The cluster approach can, therefore, be used to provide relatively accurate geometries and electronic structures, as long as care is taken to properly terminate the cluster and account for electronic charges. Weber[36] and Hoffmann[37] showed similar energetics on small and large clusters of metal oxides. A recent review highlights density functional studies on oxide materials.[38] In the work reported herein, the effect of charge distribution on the Keggin unit had to be carefully considered because the entire Keggin unit, and not individual metal centers, bears the charge. Carving clusters out of the Keggin unit, therefore, makes it difficult to appropriately assign charge. We have shown that the cluster size effect was quite large in proton affinity calculations because each Keggin unit has a −3 charge.[2] To explore any possible size effects on ammonia adsorption energies, clusters of different sizes were considered.

TABLE 1. Ammonia Adsorption Energy on Various Keggin Unit Models

cluster		adsorption energy/kJ mol^{-1}	
		tungsten	molybdenum
monomer		−56	−2
dimer		−117	−56
trimer	monodentate	−141	−103
	bidentate	−135	
	tridentate	−128	
tetramer	monodentate 1	−130	−80
	monodentate 2	−138	−100
	bidentate 1	−152	−110
	bidentate 2	−149	−100
keggin unit	monodentate 1	−151	−106
	bidentate 1	−155	
	bidentate 2	−152	−100

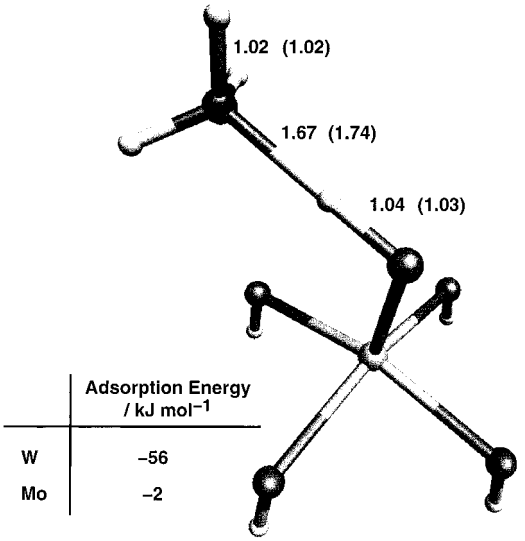

Figure 2. Ammonia adsorbed on the monomer cluster. All bond lengths are reported in angstroms. The first bond lengths reported refer to the tungsten cluster, whereas those that follow in parentheses refer to the molybdenum cluster.

Results and Discussion

We focused exclusively on two different types of Keggin HPAs, phosphotungstic and phosphomolybdic acids. The adsorption energy of ammonia is, to a significant degree, also governed by the way in which it adsorbs. In general, there are three different bonding configuration types: monodentate, bidentate, and tridentate (which refers to the number of hydrogen−oxygen bonds that exist between the ammonia and the HPA cluster). To complicate matters further, there are three distinct oxygen sites in the HPA (as discussed in the Introduction). This leads to various opportunities for ammonia adsorption that can take advantage of additional hydrogen bonding of the ammonium ion with the Keggin unit.

We began our current studies by investigating the effect of cluster size on the computed ammonia adsorption energies. The adsorption energy of ammonia bound monodentate to the monomer, dimer, trimer, and tetramer tungsten HPA clusters were calculated to be −56, −117, −141, and −130 kJ mol^{-1}, respectively, as shown in Table 1. The adsorption energy on the monomer cluster is significantly lower and is likely due to the fact that the only available adsorption site is the terminal oxygen (Figure 2). The bridging oxygen site is used for all other clusters, as illustrated in Figure 3 for the dimer cluster, because it is the more favorable proton site.[2] The changes in the adsorption energy become much smaller as one moves beyond the dimer cluster, indicating a relatively weak cluster-size effect.

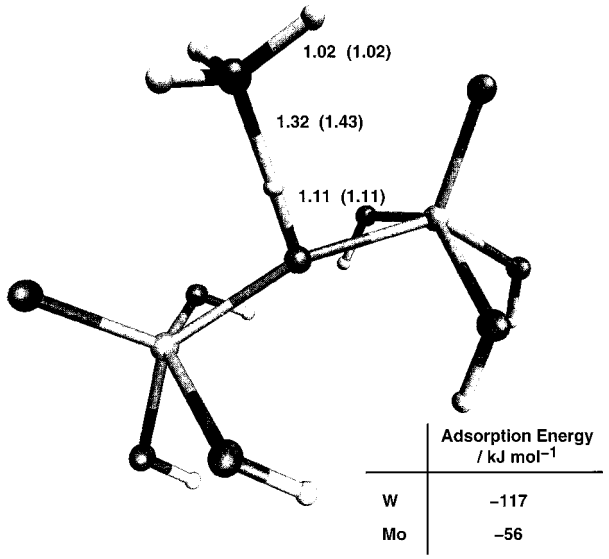

Figure 3. Ammonia adsorbed on the dimer cluster. All bond lengths are reported in angstroms. The first bond lengths reported refer to the tungsten cluster, whereas those that follow in parentheses refer to the molybdenum cluster.

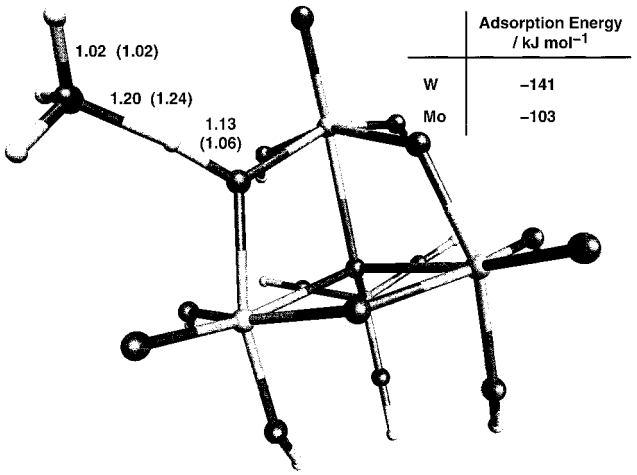

Figure 4. Ammonia adsorbed on the trimer cluster in a monodentate position. All bond lengths are reported in angstroms. The first bond lengths reported refer to the tungsten cluster, whereas those that follow in parentheses refer to the molybdenum cluster.

This differs from the results of our proton-affinity calculations,[2] in which we had a negatively charged cluster interacting with a positively charged proton to form a neutral system. The distribution of negative charge on the cluster varied greatly as the cluster size increased. In the present ammonia calculations, the charge on the cluster is neutral because an acidic proton is already adsorbed to the surface before the ammonia interactions are computed. This leads to more consistent values as the cluster size increases. The results of the optimized structures and energies are shown in Figures 4, 5, and 6 for the trimer, tetramer, and Keggin unit, respectively.

Ammonia bound monodentate on the trimer cluster adsorbs without proton transfer, as seen in Figure 4. The O−H$^+$ bond increases slightly to 1.13 Å but remains intact. The distance between the proton and the adsorbed ammonia is 1.20 Å. The calculated adsorption energy is −141 kJ mol^{-1}.

On the tetramer, there are two possible monodentate adsorption positions for the ammonia. The first position (monodentate 1) corresponds to the bridging oxygen that is located directly over a central oxygen atom. This is the same site that was used

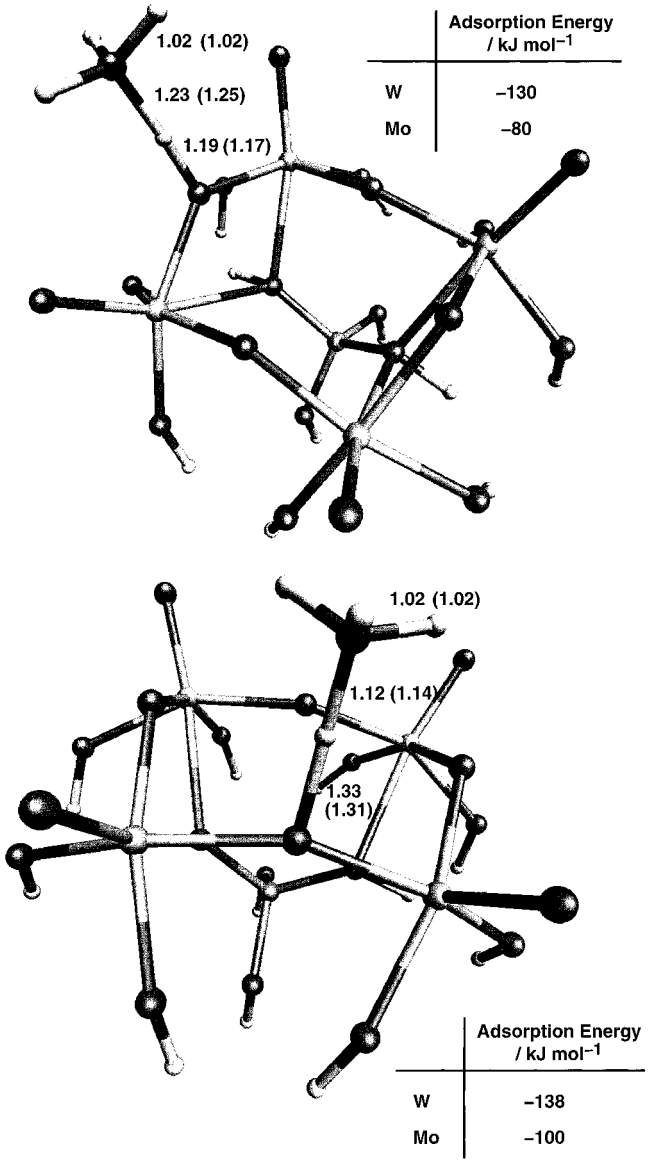

Figure 5. Ammonia adsorbed on the tetramer cluster in the monodentate orientation, (a) bridging position one and (b) bridging position two. All bond lengths are reported in angstroms. The first bond lengths reported refer to the tungsten clusters, whereas those that follow in parentheses refer to the molybdenum clusters.

in the trimer calculations. Ammonia adsorbs with a partial degree of proton transfer whereby the $O-H^+$ (1.19 Å) and the $N-H^+$ (1.23 Å) bond distances are nearly equivalent. The predicted adsorption energy of ammonia at monodentate site 1 on the tetramer cluster is -130 kJ mol^{-1}. The second monodentate adsorption site on the tetramer cluster (monodentate 2) involves a bridging oxygen that is not located directly over a central oxygen atom. Adsorption at this site tends to result in a higher degree of proton transfer in which the $O-H^+$ bond length is 1.33 Å and the $N-H^+$ bond length is 1.12 Å (Figure 5b). The predicted energy of adsorption is -131 kJ mol^{-1}, which is slightly stronger than that for chemisorption at monodentate site 1.

The full Keggin structure was also examined to complete the analysis for the chemisorption of ammonia at the monodentate positions. Once again, a partial transfer of the proton resulted in the $O-H^+$ and $N-H^+$ distances of 1.13 Å and 1.20 Å, respectively (Figure 6). The adsorption energy was -151 kJ mol^{-1} for tungsten.

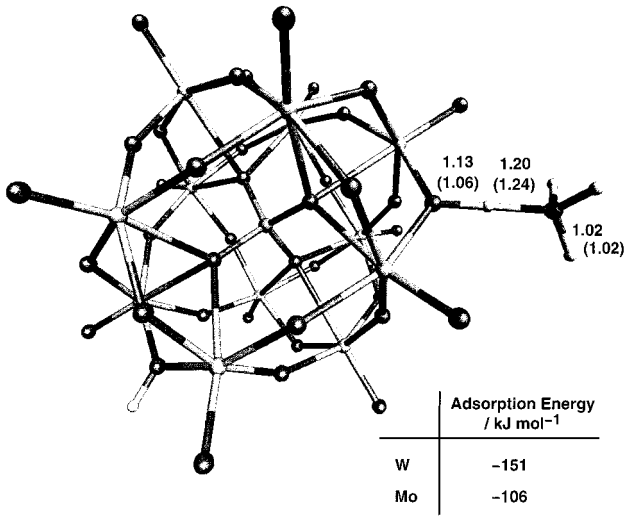

Figure 6. Ammonia adsorbed on the Keggin unit. One molecule of ammonia has been adsorbed onto a protonated Keggin structure. All bond lengths are reported in angstroms. The first bond lengths reported refer to the tungsten Keggin unit, whereas those that follow in parentheses refer to the molybdenum Keggin unit.

A careful analysis of the structural and energetic results revealed a relatively flat potential-energy surface for proton transfer with only about 10 kJ mol^{-1} difference between a fully protonated ammonium ion and a bound ammonia species on the trimer model. This result is not unique to heteropolyacids. Gale showed that incomplete proton-transfer in zeolites results in a local minimum in potential energy.[15] The formation of ammonium in zeolites has been discussed by van Santen et al.[7,39] Ammonia that is adsorbed on small clusters without the stabilizing effects of additional hydrogen bonding does not lead to the formation of an ammonium. In the presence of additional hydrogen bonding, however, ammonium readily forms via proton transfer. In addition to ammonia adsorption, methanol also shows enhanced proton transfer with additional hydrogen bonding. Bates et al.[40] estimated the proton transfer between a zeolite cluster and adsorbed methanol to be ~5.7 kJ mol^{-1}, near our value of 10 kJ mol^{-1} for the heteropolyacid system. Allavena et al.[41] reported that the hydrogen-bonded ammonia interaction for a monodentate system was more stable than the ammonium−zeolite interaction on a zeolite cluster. They concluded that the model of the ammonia interaction with the zeolite must need revising because ammonium is observed experimentally. This conclusion is supported by others.[7]

In a similar vein to the zeolite studies, we examined various adsorption configurations of ammonia on the heteropolyacid clusters. We know from experimental reports that an ammonium ion is formed when ammonia is introduced to the heteropolyacid.[42−44] Clearly, the monodentate model does not provide the entire picture of ammonia adsorption on Keggin-type heteropolyacids. Figure 7 shows ammonia-adsorbed bidentate on a tungsten trimer cluster. The adsorption energy of -135 kJ mol^{-1} is approximately equal to that of the ammonia-bound monodentate on the tungsten trimer cluster. In this bidentate arrangement, however, we observe that the proton transfers to the ammonia.

Additional bidentate calculations were performed using the tetramer cluster. Figure 8a shows the optimized structure for ammonia adsorbed between a terminal-oxygen and a bridging-oxygen site. The adsorption energy is -152 kJ mol^{-1}. Ammonia adsorbed between two bridging oxygens leads to a very similar energy of -149 kJ mol^{-1}, as seen in Figure 8b. These adsorption energies for ammonia on the tetramer cluster are 22 and 11 kJ

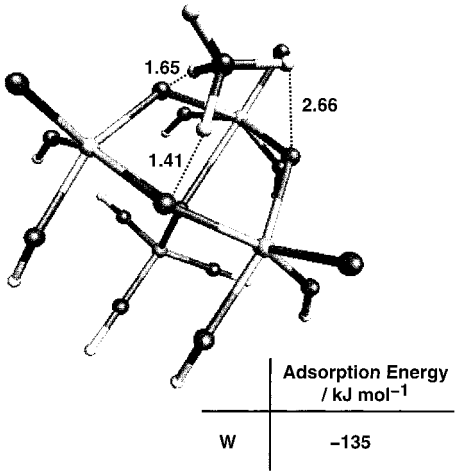

Figure 7. Bidentate adsorption of ammonia on the tungsten trimer cluster. Bond lengths are in angstroms.

mol^{-1} greater than those for the monodentate species. The additional stabilization appears to facilitate proton transfer as the ammonium intermediate is the most stable structure for all bidentate arrangements.

To remove any cluster size effects, we calculated the adsorption energies of ammonia in the bidentate configuration on the full Keggin unit for both W and Mo HPAs as illustrated in Figure 9. Figure 9a shows the bidentate adsorption of ammonia between a terminal and a bridging oxygen. The adsorption of ammonia between two bridging oxygens are shown in Figure 9b for a tungsten and molybdenum HPA. The results for these calculations agree with the trends in the binding energies computed for the smaller clusters, i.e., tungsten HPAs have computed ammonia binding energies approximately 40−50 kJ mol^{-1} higher than the molybdenum HPAs. The bidentate adsorption mode promoted complete proton transfer to the ammonia as observed on the tetramer clusters.

Another possible adsorption mode of ammonia on the Keggin structure involves the tridentate interaction. The results for the tridentate-bound ammonia on the trimer cluster are shown in Figure 10. This model was based on an arrangement suggested by Bielanski et al.[44] These results indicate that the adsorption energy decreases from −135 to −128 kJ mol^{-1} for the formation of the ammonium ion in the bidentate and tridentate geometry, respectively. This decrease in the adsorption energy may be due to repulsive interactions between the Keggin unit and the ammonium ion.

One final point that should be considered when modeling heteropolyacids is the interaction of neighboring Keggin units in a bulk solid. The clusters used here are analogous to well-dispersed Keggin units isolated on a support. In the bulk system, neighboring Keggin units may aid in stabilizing an ammonia that is bound in a monodentate manner by providing additional hydrogen bonding. This additional stabilization from neighboring Keggin units should aid in proton transfer to form an ammonium ion.

Our initial goal in pursuing computational studies on heteropolyacids was to demonstrate that solid acid strength could be ranked by the combination of experimental and theoretical methods. Heteropolyacids are good materials to pursue this goal because merely changing the transition metal from tungsten to molybdenum remarkably decreases the acid strength of the catalysts.[2] However, very little difference is observed in the structure of the Keggin unit, other than slight changes in bond lengths. This allows for easy comparison of the two heteropoly-

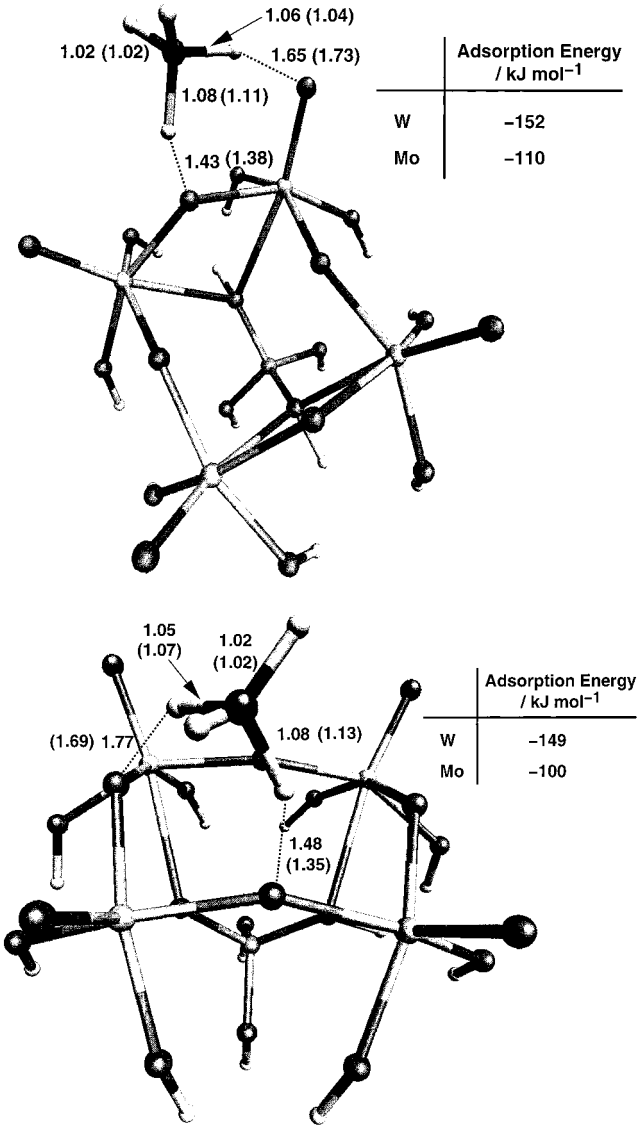

Figure 8. Ammonia adsorbed on the tetramer cluster in the bidentate form. (a) Ammonia adsorbed between a terminal oxygen and a bridging oxygen. (b) Ammonia adsorbed between the two types of bridging oxygens. All bond lengths are reported in angstroms. The first bond lengths reported refer to the tungsten clusters, whereas those that follow in parentheses refer to the molybdenum clusters.

acids by density functional methods. We previously reported that molybdenum heteropolyacids had higher proton affinities than their tungsten counterparts, thus indicating that the molybdenum heteropolyacids were weaker acids.[2] By comparing ammonia adsorption energies over molybdenum and tungsten heteropolyacids, we can begin to examine relative acidites. In general, stronger acids will bind with ammonia more strongly than weaker acids. If we compare the values in Table 1 for the tungsten and molybdenum heteropolyacids, we observe that the adsorption energies are always stronger on the tungsten cluster than on the analogous molybdenum cluster. In the monomer calculation, tungsten had an adsorption energy of −56 kJ mol^{-1}, whereas molybdenum had a value of −2 kJ mol^{-1}. This difference, of approximately 50 kJ mol^{-1} between the tungsten and the molybdenum adsorption energies, is consistent for all of the clusters and adsorption configurations that were compared. The calculation of ammonia bound to the trimer in a monodentate arrangement gave −141 and −103 kJ mol^{-1} for tungsten and molybdenum, respectively. Changing the adsorption mode had little effect on the relative difference in adsorption energy

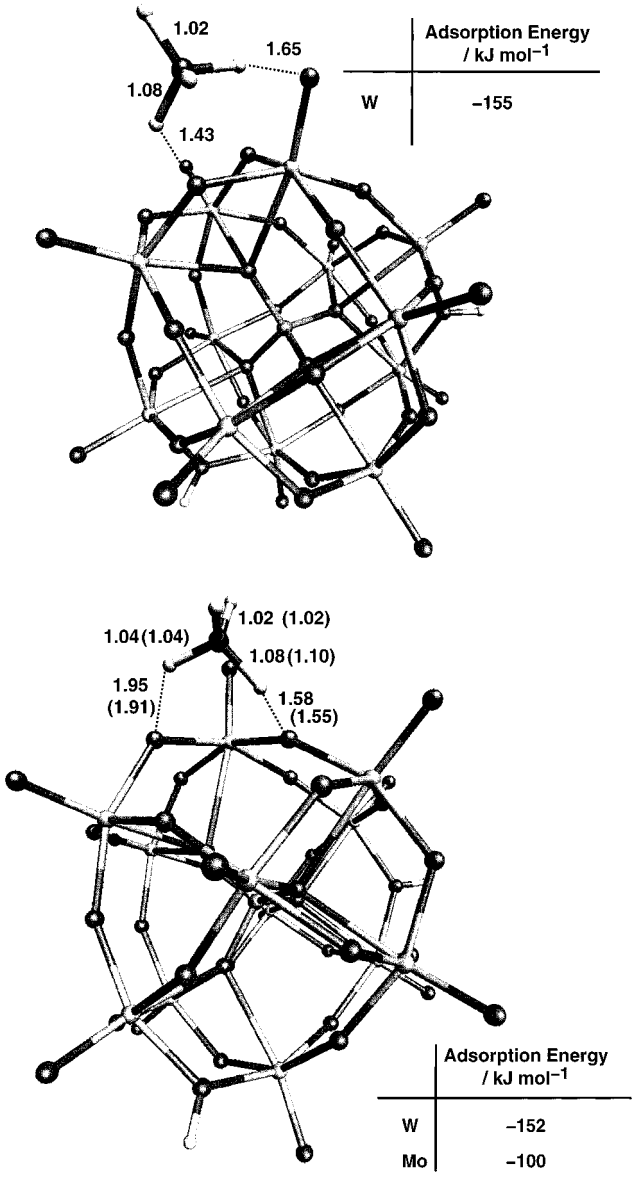

Figure 9. Bidentate adsorption of ammonia on the Keggin unit. (a.) Ammonia adsorbed between a terminal oxygen and a bridging oxygen on a tungsten Keggin unit. (b.) Ammonia adsorbed between the two types of bridging oxygens on a molybdenum and tungsten Keggin unit. All bond lengths are reported in angstroms. The first bond lengths reported refer to the tungsten Keggin unit, whereas those that follow in parentheses refer to the molybdenum Keggin unit.

between the W and Mo clusters. The computation of ammonia bound to the tetramer in a bidentate mode yielded differences of 42 and 49 kJ mol^{-1} between the tungsten and molybdenum clusters for bidentate 1 and bidentate 2 sites, respectively. This shows that heteropolyacids composed of tungsten are stronger acids than are those composed of molybdenum, which is consistent with results seen in the liquid phase.[19]

The calculation of gas-phase proton affinity as a measure of acid strength is applicable in some circumstances; however, for a more correct measure of acid strength, a base is needed to bind the acidic proton. One advantage of computing ammonia adsorption energies rather than gas-phase proton affinities is that we can directly compare the results with the measured experimental values. The proton affinities of solids are difficult to measure experimentally using an affinity distribution.[45,46] Computed ammonia adsorption energies can be compared to results from ammonia sorption microcalorimetry. We previously reported values for ammonia sorption on anhydrous tungsten

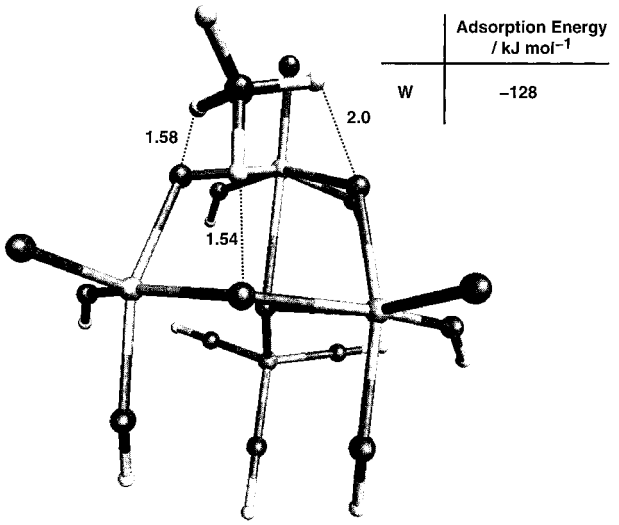

Figure 10. Tridentate adsorption of ammonia on the tungsten trimer cluster. Bond lengths are in angstroms.

heteropolyacids to be about −150 kJ mol^{-1}.[2] Others have shown similar results for the heat of ammonia sorption on tungsten-based Keggin units.[47,48] Our computational results are in very good agreement with the experimental values. Each of the larger clusters (trimer, tetramer, or Keggin unit) and the different adsorption configurations (monodentate or bidentate) used in our model generated results that were within 20 kJ mol^{-1} of the sorption energies obtained by experiment. Similarly, we obtained good agreement between the adsorption energy of ammonia and the heats of ammonia sorption for the molybdenum containing heteropolyacid. Our previously reported results showed ammonia sorption energies of about −120 kJ mol^{-1} for an anhydrous molybdenum Keggin unit, which is close to the value of −106 kJ mol^{-1} computed for the ammonia bound to the Keggin unit in a monodentate adsorption mode. Zeolites have also been effectively characterized using these microcalorimetric experiments.[49−51] A heat of adsorption of ammonia near −145 kJ mol^{-1} was obtained on strong acid zeolites such as H−ZSM-5. As mentioned previously, in our calculations of ammonia adsorption energy, we obtained a value of about −150 kJ mol^{-1} for the adsorption energy of ammonia on the tungsten heteropolyacid, which is the stronger acid of the two heteropolyacids investigated.

We should note that simple agreement of the computed heat of adsorption of ammonia on the Keggin HPAs with the measured heat of ammonia sorption does not indicate that all ammonium cations in a heteropolyacid system are bound in monodentate or bidentate configurations. As ammonia is introduced into the bulk HPA, an ammonium salt is formed. The ammonium cation will not be interacting with only one Keggin unit in isolation but with many Keggin units in various binding configurations.

Ammonia is one of the simplest molecules used to study interactions with acid sites in solids. Indeed, it is the most studied of all of the basic probe molecules. Other probe molecules, such as pyridine, can provide insight into the acid character of solids.[12] Microcalorimetry experiments of pyridine on H-ZSM-5 yielded heats of adsorption near 200 kJ mol^{-1}.[50] To begin to address the issue of using more complex bases in modeling heteropolyacids, we examined the adsorption of pyridine in a monodentate position on both the tungsten and the molybdenum tetramer clusters. The results are shown in Figure 11. Adsorption energies of −180 and −125 kJ mol^{-1} were obtained for the tungsten and molybdenum clusters,

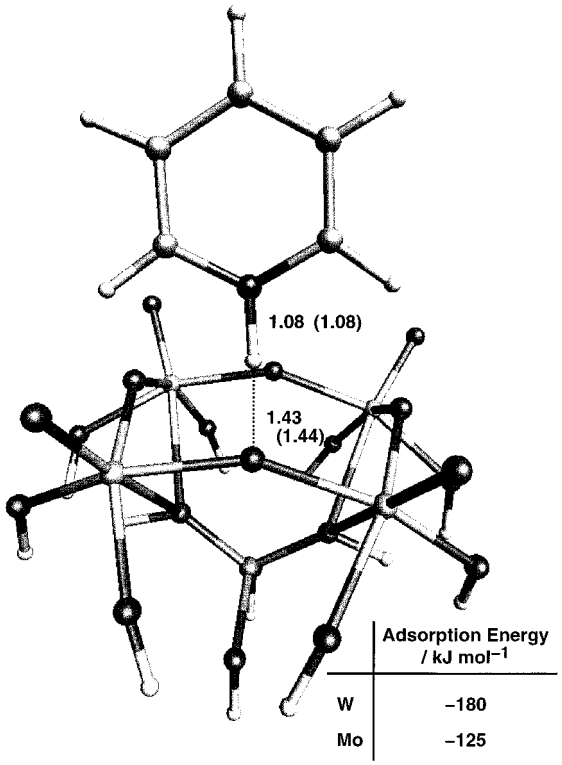

Figure 11. Adsorption of pyridine on the tungsten and molybdenum tetramer clusters. All bond lengths are reported in angstroms. The first bond lengths reported refer to the tungsten clusters, whereas those that follow in parentheses refer to the molybdenum clusters.

respectively. These results are consistent with the results for ammonia. The adsorption energies were larger for pyridine than for the ammonia on the Keggin structures, which was anticipated, given the relative basicity of pyridine relative to ammonia and the previous results from microcalorimetry experiments on zeolites. Unlike the ammonia monodentate species, complete proton transfer was obtained using the pyridine. This is most likely due to the greater stabilization provided by the increase in size from ammonia to pyridine. In addition, the proton affinity of pyridine is greater than that of ammonia, providing a greater driving force for proton transfer in pyridine adsorption.

Conclusions

In this paper, we have shown that density functional theory can be used to differentiate acid strength between phosphotungstic and phosphomolybdic acids through the calculation of ammonia-adsorption energy. Phosphotungstic acid had larger ammonia-adsorption energies than phosphomolybdic acid, indicating that the former is the stronger acid. This is consistent with the suggested acid strengths determined from microcalorimetry and reactivity.[2] Proton transfer was not readily observed for models in which ammonia was adsorbed monodentate to the Keggin structure. However, when a bidentate species was modeled to include additional stabilization due to hydrogen bonding, complete proton transfer from the Keggin unit to the ammonia, to form an ammonium ion and a negatively charged heteropolyacid surface, was observed. In general, the bidentate species had stronger adsorption energies than their monodentate counterparts due to the extra stabilization of the additional hydrogen bond. We were able to optimize both the monodentate and the bidentate ammonia species on the full Keggin unit. Finally, a calculation of the pyridine adsorption energy on the heteropolyacid gave higher values than those given for ammonia adsorption, correlating to microcalorimetry results on acidic zeolites.

Acknowledgment. Funding for this work was provided by a graduate traineeship grant from the National Science Foundation in Environmentally Conscious Chemical Manufacturing (Grant No. GER9452654). Additional funding for this work was provided by the Virginia Academic Enhancement Program.

References and Notes

(1) Corma, A. *Chem. Rev.* **1995**, *95*, 559.
(2) Bardin, B. B.; Bordawekar, S. V.; Neurock, M.; Davis, R. J. *J. Phys. Chem. B* **1998**, *102*, 10 817.
(3) Kramer, G. J.; van Santen, R. A. *J. Am. Chem. Soc.* **1993**, *115*, 2887.
(4) Chandra, A. K.; Goursot, A.; Fajula, F. *J. Mol. Catal. A: Chem.* **1997**, *119*, 45.
(5) Gonzales, N. O.; Bell, A. T.; Chakraborty, A. K. *J. Phys. Chem. B* **1997**, *101*, 10 058.
(6) Sauer, J. *Chem. Rev.* **1989**, *89*, 199.
(7) van Santen, R. A.; Kramer, G. J. *Chem. Rev.* **1995**, *95*, 637.
(8) Blaszkowski, S. R.; van Santen, R. A. *Top. Catal.* **1997**, *4*, 145.
(9) Zygmunt, S. A.; Mueller, R. M.; Curtiss, L. A.; Iton, L. E. *THEOCHEM* **1998**, *430*, 9.
(10) Nicholas, J. B. *Top. Catal.* **1997**, *4*, 157.
(11) Kyrlidis, A.; Cook, S. J.; Chakraborty, A. K.; Bell, A. T.; Theodorou, D. N. *J. Phys. Chem.* **1995**, *99*, 1505.
(12) Gorte, R. J.; White, D. *Top. Catal.* **1997**, *4*, 57.
(13) Greatbanks, S. P.; Hillier, I. H.; Sherwood, P. *J. Comput. Chem.* **1997**, *18*, 562.
(14) Teunissen, E. H.; Jansen, A. P. J.; van Santen, R. A. *J. Phys. Chem.* **1995**, *99*, 1873.
(15) Gale, J. D. *Top. Catal.* **1996**, *3*, 169.
(16) Pope, M. T. *Heteropoly and Isopoly Oxometalates*; Springer-Verlag: Berlin, 1983.
(17) Moffat, J. B. *J. Mol. Catal.* **1984**, *26*, 385.
(18) Viswanathan, B. *Indian J. Chem.* **1990**, *29A*, 509.
(19) Okuhara, T., Mizuno, N., Misono, M. *Adv. Catal.* **1996**, *41*, 113.
(20) Na, K.; Okuhara, T.; Misono, M. *Chem. Lett.* **1993**, 1141.
(21) Essayem, N.; Coudurier, G.; Fournier, M.; Vedrine, J. C. *Catal. Lett.* **1995**, *34*, 223.
(22) Bardin, B. B.; Davis, R. J. *Top. Catal.* **1998**, *6*, 77.
(23) Misono, M. *Catal. Rev.—Sci. Eng.* **1987**, *30*, 269.
(24) Kozhevnikov, I. V. *Russ. Chem. Rev.* **1987**, *56*, 1417.
(25) Lee, K. Y.; Mizuno, N.; Okuhara, T.; Misono, M. *Bull. Chem. Soc. Jpn.* **1989**, *62*, 1731.
(26) Kozhevnikov, I. V. *Catal. Lett.* **1995**, *34*, 213.
(27) Ziegler, T. *Chem. Rev.* **1991**, *91*, 651.
(28) Neurock, M. *Appl. Catal., A* **1997**, *160*, 169.
(29) Amsterdam Density Functional 2.3.0. Theoretical Chemistry; Vrije Universiteit: Amsterdam.
(30) Baerends, E. J.; Ellis, D. E.; Ros, P. *Chem. Phys.* **1973**, *2*, 41.
(31) Te Velde, G.; Baerends, E. J. *J. Comput. Phys.* **1992**, *99*, 84.
(32) Vosko, S. H.; Wilk, L.; Nusair, M. *Can. J. Phys.* **1980**, *58*, 1200.
(33) Becke, A. D. *Phys. Rev. A* **1988**, *38*, 3098.
(34) Becke, A. D. *ACS Symp. Ser.* **1989**, *394*, 165.
(35) Perdew, J. P. *Phys. Rev. B* **1986**, *33*, 8822.
(36) Weber, R. S. *J. Phys. Chem.* **1994**, *98*, 2999.
(37) Schiott, B.; Jorgensen, K. A.; Hoffmann, R. *J. Phys. Chem.* **1991**, *95*, 2297.
(38) Neyman, K. M.; Pacchioni, G.; Rosch, N. *Theor. Comput. Chem.* **1996**, *4*, 569.
(39) Teunissen, E. H.; van Duijneveldt, F. B.; van Santen, R. A. *J. Phys. Chem.* **1992**, *96*, 366.
(40) Bates, S.; Dwyer, J. *J. Mol. Struct.* **1994**, *306*, 57.
(41) Allavena, M.; Kassab, E.; Evleth, E. *J. Mol. Struct.* **1994**, *325*, 85.
(42) Southward, B. W. L.; Vaughan, J. S.; O'Connor, C. T. *J. Catal.* **1995**, *153*, 293.
(43) Essayem, N.; Frety, R.; Coudurier, G.; Vedrine, J. C. *J. Chem. Soc., Faraday Trans.* **1997**, *93*, 3243.
(44) Bielanski, A.; Malecka, A.; Kubelkova, L. *J. Chem. Soc., Faraday Trans.* **1989**, *85*, 2847.
(45) Adachi, M.; Contescu, C.; Schwarz, J. A. *J. Catal.* **1996**, *158*, 411.
(46) Contescu, C.; Popa, V. T.; Miller, J. B.; Ko, E. I.; Schwarz, J. A. *J. Catal.* **1995**, *157*, 244.
(47) Jozefowicz, L. C.; Karge, H. G.; Vasilyeva, E.; Moffat, J. B. *Microporous Mater.* **1993**, *1*, 313.
(48) Kapustin, G. I.; Brueva, T. R.; Klyachko, A. L.; Timofeeva, M. N.; Kulikov, S. M.; Kozhevnikov, I. V. *Kinet. Katal.* **1990**, *31*, 896.
(49) Farneth, W. E., Gorte, R. J. *Chem. Rev.* **1995**, *95*, 615.
(50) Parrillo, D. J.; Gorte, R. J. *J. Phys. Chem.* **1993**, *97*, 8786.
(51) Parrillo, D. J., Lee, C., Gorte, R. J. *Appl. Catal. A* **1994**, *110*, 67.